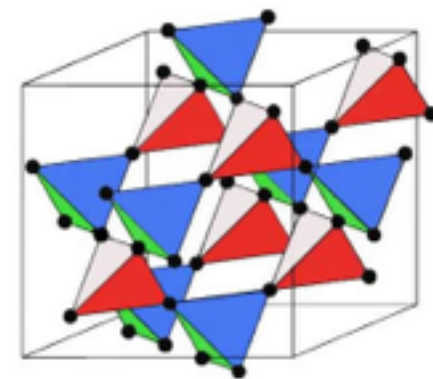


Competing orders and topological excitations in spin-1 pyrochlore antiferromagnets

Gang Chen
Department of Physics
Fudan University

(currently on a sabbatical leave to University of Hong Kong)



PHYSICAL REVIEW B **98**, 045109 (2018)

Competing phases and topological excitations of spin-1 pyrochlore antiferromagnets

Fei-Ye Li^{1,2} and Gang Chen^{1,2,3,4,*}

¹*State Key Laboratory of Surface Physics and Department of Physics, Fudan University, Shanghai 200433, China*

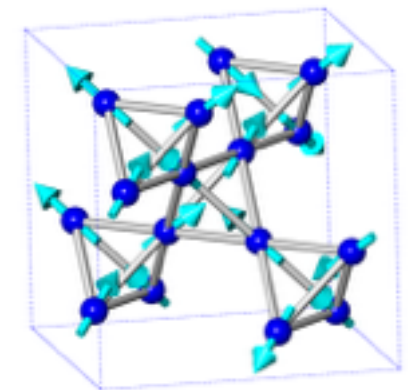
²*Center for Field Theory and Particle Physics, Fudan University, Shanghai 200433, China*

³*Institute for Nanoelectronic Devices and Quantum Computing, Fudan University, Shanghai, 200433, China*

⁴*Collaborative Innovation Center of Advanced Microstructures, Nanjing University, Nanjing 210093, China*

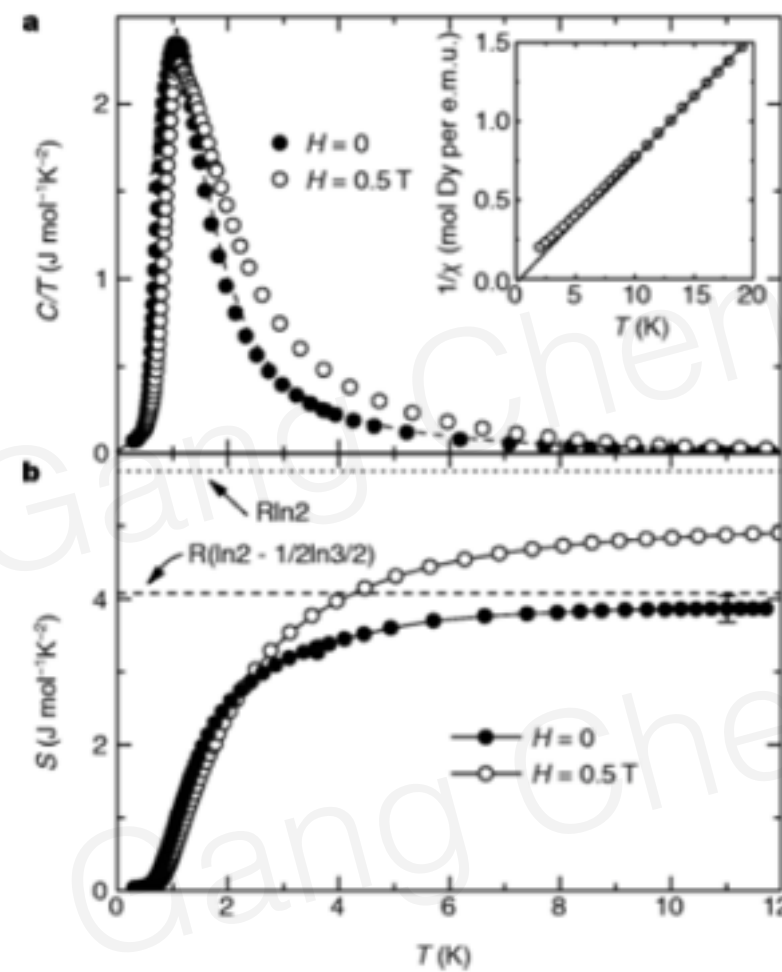
Fei-Ye Li
Fudan

Fei-Ye Li, GC, PhysRevB 98, 045109 (2018)



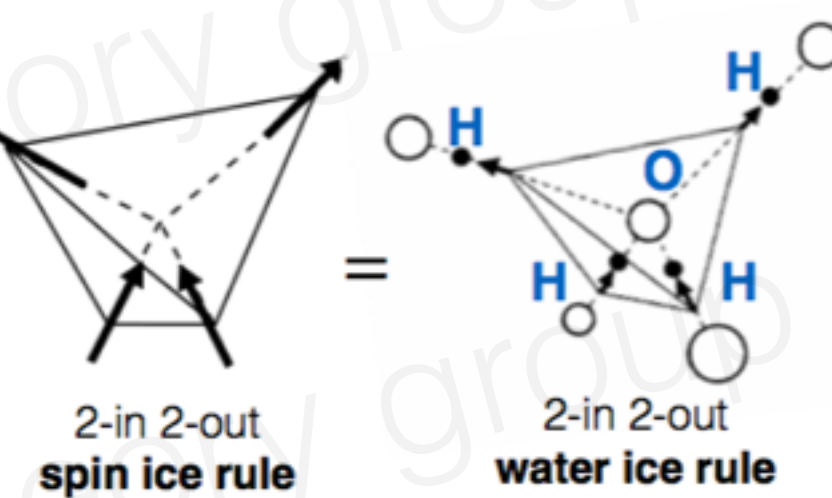
Everlasting success of spin-1/2 pyrochlores

Dy₂Ti₂O₇



Pauling entropy in spin ice

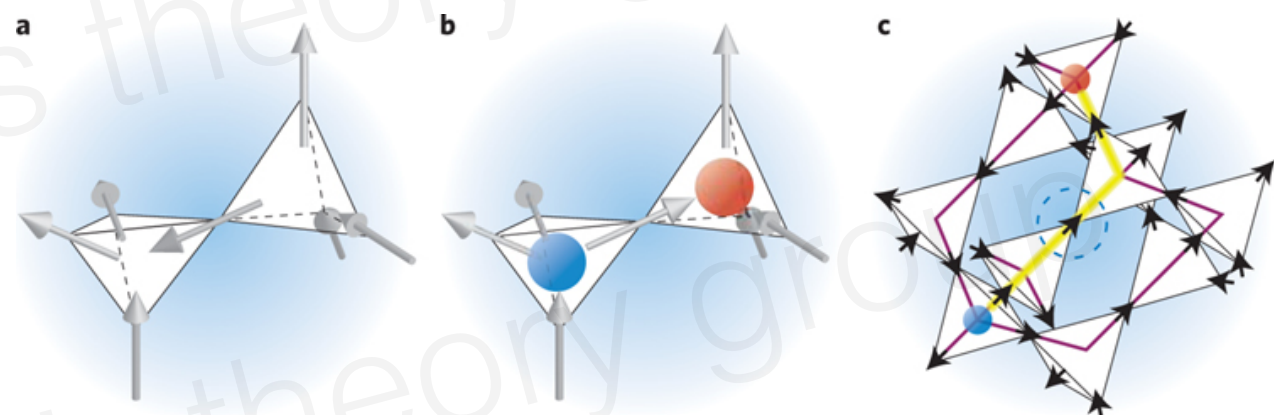
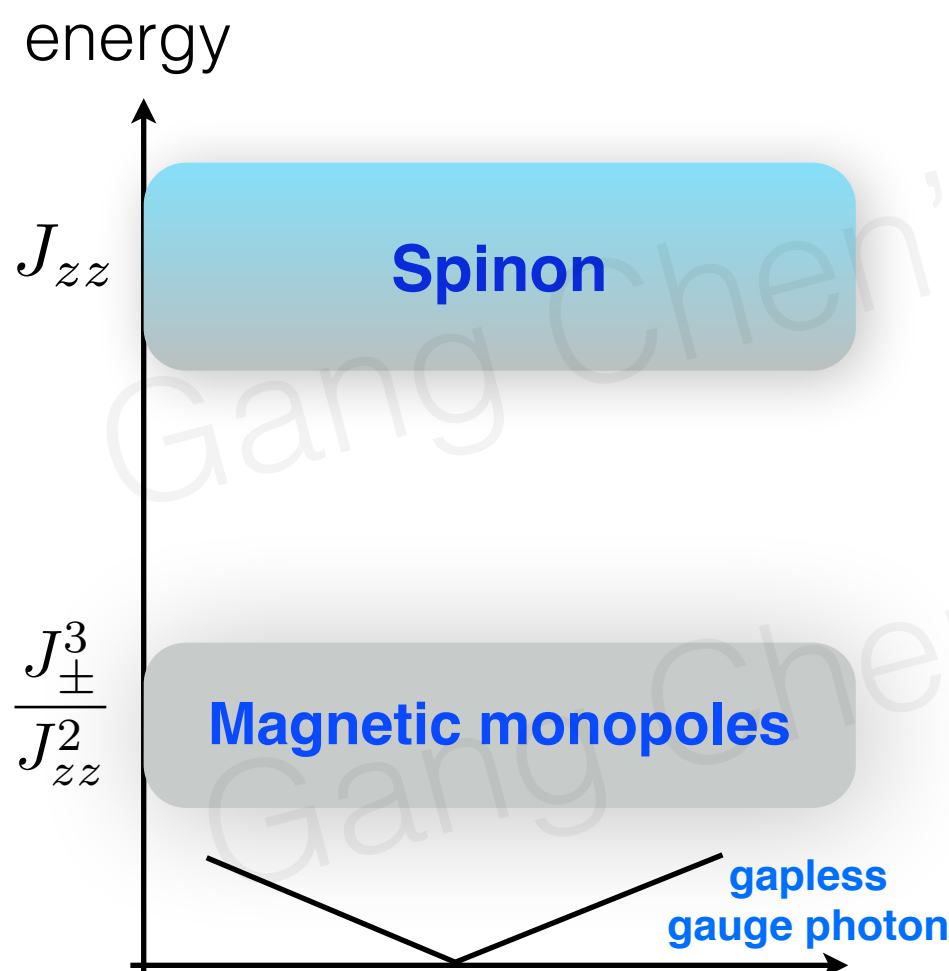
Classical spin ice



Ramirez, etc, Nature 1999,
Gingras, etc, Science, 2009
Castelnovo, Moessner, etc, Nature 2008

Everlasting success of spin-1/2 pyrochlores

Quantum spin ice,
Quantum spin liquid



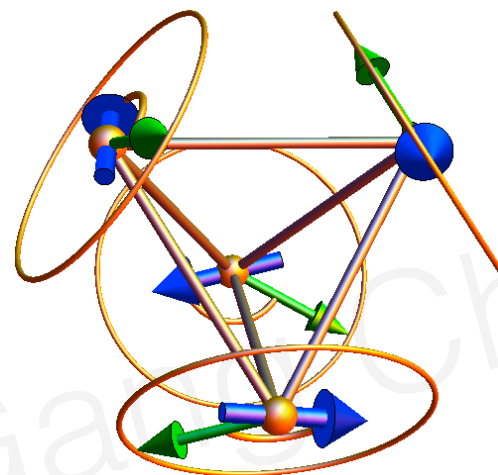
Figs from Moessner&Schiffer,2009

Spinon deconfinement

Gingras, Gaulin, Balents, Savary, SB Lee, GC,

Everlasting success of spin-1/2 pyrochlores

Order by quantum disorder



XY pyrochlore

Kate Ross, Bruce Gaulin, etc

$\text{Er}_2\text{Ti}_2\text{O}_7$ Hamiltonian: The effective $S = 1/2$ description applies to $\text{Er}_2\text{Ti}_2\text{O}_7$ below about 74 K [2, 11]. Nearest-neighbor exchange dominates, for which the Hamiltonian is constrained by symmetry to the form [9]

$$H = \sum_{\langle ij \rangle} \left[J_{zz} S_i^z S_j^z - J_{\pm} (S_i^+ S_j^- + S_i^- S_j^+) \right. \\ \left. + J_{\pm\pm} [\gamma_{ij} S_i^+ S_j^+ + \gamma_{ij}^* S_i^- S_j^-] \right. \\ \left. + J_{z\pm} [S_i^z (\zeta_{ij} S_j^+ + \zeta_{ij}^* S_j^-) + i \leftrightarrow j] \right], \quad (6)$$

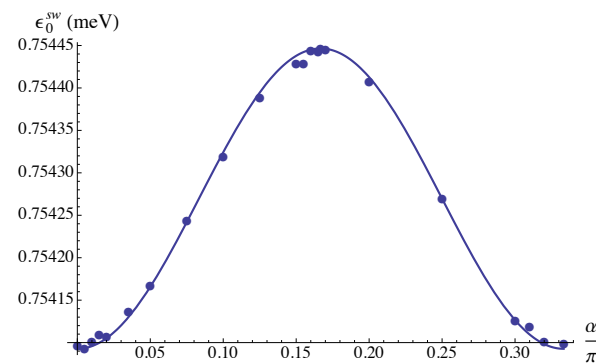
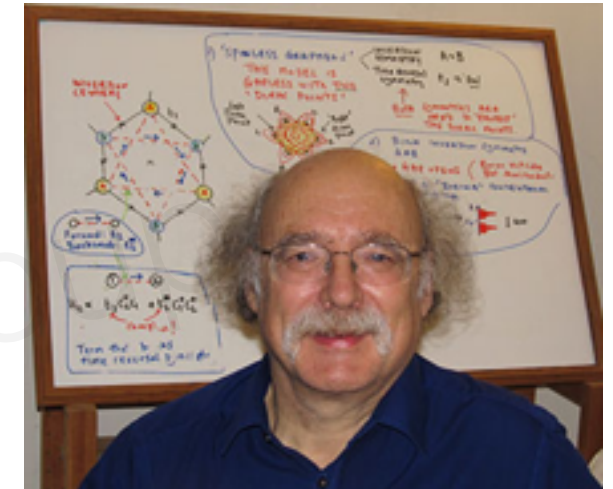


FIG. 2. Zero-point fluctuation energy ϵ_0^{sw} in the classically degenerate manifold parametrized by α . The peak-to-peak energy is $\lambda \approx 3.5 \cdot 10^{-4}$ meV.

The difference between spin-1/2 and spin-1

Due to Berry phase effect, spin-1/2 chain is gapless, spin-1 Heisenberg chain is gapped.



Duncan Haldane
Nobel Prize 2016



$$\bullet - \bullet = \frac{1}{\sqrt{2}} (| \uparrow \downarrow \rangle - | \downarrow \uparrow \rangle)$$

$$\textcircled{\bullet} = |+\rangle\langle \uparrow\uparrow| + |0\rangle \frac{\langle \uparrow\downarrow | + \langle \downarrow\uparrow |}{\sqrt{2}} + |-\rangle\langle \downarrow\downarrow|$$

S=1 chain

AKLT state

Building degree of freedom is S=1, but at there is S=1/2 edge state.

Spin-1 pyrochlores

materials	magnetic ions	Θ_{CW}	magnetic transitions	magnetic structure
NaCaNi ₂ F ₇	Ni ²⁺ (3d ⁸)	-129K	glassy transition at 3.6K	spin glass
Y ₂ Ru ₂ O ₇	Ru ⁴⁺ (4d ⁴)	-1250K	AFM transition at 76K	canted AFM $Q = 0$
Tl ₂ Ru ₂ O ₇	Ru ⁴⁺ (4d ⁴)	-956K	structure transition at 120K	gapped paramagnet
Eu ₂ Ru ₂ O ₇	Ru ⁴⁺ (4d ⁴)	-	Ru order at 118K	Ru order
Pr ₂ Ru ₂ O ₇	Ru ⁴⁺ (4d ⁴), Pr ³⁺ (4f ²)	-224K	Ru AFM order at 162K	Ru AFM order
Nd ₂ Ru ₂ O ₇	Ru ⁴⁺ (4d ⁴), Nd ³⁺ (4f ³)	-168K	Ru AFM order at 143K	Ru AFM order
Gd ₂ Ru ₂ O ₇	Ru ⁴⁺ (4d ⁴), Gd ³⁺ (4f ⁷)	-10K	Ru AFM order at 114K	Ru AFM order $Q = 0$
Tb ₂ Ru ₂ O ₇	Ru ⁴⁺ (4d ⁴), Tb ³⁺ (4f ⁸)	-16K	Ru AFM order at 110K	Ru AFM order $Q = 0$
Dy ₂ Ru ₂ O ₇	Ru ⁴⁺ (4d ⁴), Dy ³⁺ (4f ⁹)	-10K	Ru AFM order at 100K	Ru AFM order
Ho ₂ Ru ₂ O ₇	Ru ⁴⁺ (4d ⁴), Ho ³⁺ (4f ¹⁰)	-4K	Ru AFM order at 95K	Ru FM order $Q = 0$
Er ₂ Ru ₂ O ₇	Ru ⁴⁺ (4d ⁴), Er ³⁺ (4f ¹¹)	-16K	Ru AFM order at 92K	Ru AFM order $Q = 0$
Yb ₂ Ru ₂ O ₇	Ru ⁴⁺ (4d ⁴), Yb ³⁺ (4f ¹³)	-	Ru AFM order at 83K	Ru AFM order
Y ₂ Mo ₂ O ₇	Mo ⁴⁺ (4d ²)	-200K	Mo spin glass at 22K	Mo spin glass
Lu ₂ Mo ₂ O ₇	Mo ⁴⁺ (4d ²)	-160K	Mo spin glass at 16K	Mo spin glass
Tb ₂ Mo ₂ O ₇	Mo ⁴⁺ (4d ²), Tb ³⁺ (4f ⁸)	20K	spin glass at 25K	spin glass

Candidate spin-1 pyrochlore materials

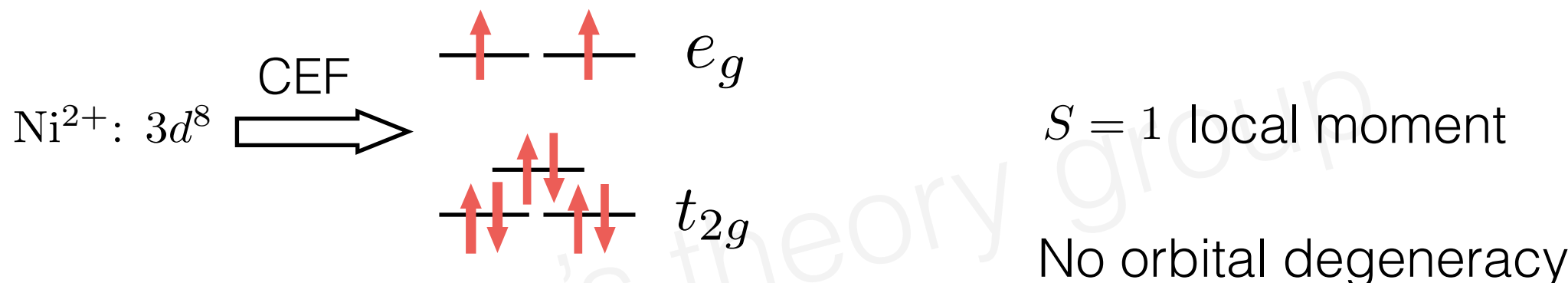
References are listed in PRB 98, 045109

21 Sc 44.956	22 Ti 47.867	23 V 50.942	24 Cr 51.996	25 Mn 54.938	26 Fe 55.845	27 Co 58.933	28 Ni 58.693	29 Cu 63.546	30 Zn 65.38
39 Y 88.906	40 Zr 91.224	41 Nb 92.906	42 Mo 95.95	43 Tc (98)	44 Ru 101.07	45 Rh 102.91	46 Pd 106.42	47 Ag 107.87	48 Cd 112.41
71 Lu 174.97	72 Hf 178.49	73 Ta 180.95	74 W 183.84	75 Re 186.21	76 Os 190.23	77 Ir 192.22	78 Pt 195.08	79 Au 196.97	80 Hg 200.59
103 Lr (266)	104 Rf (267)	105 Db (268)	106 Sg (269)	107 Bh (270)	108 Hs (277)	109 Mt (278)	110 Ds (281)	111 Rg (282)	112 Cn (285)

Model Hamiltonian

Local moment physics of the Ni^{2+} ion in $\text{NaCaNi}_2\text{F}_7$

J. W. Krizan and R. J. Cava
PRB 92, 014406 (2015)



Generic Model Hamiltonian

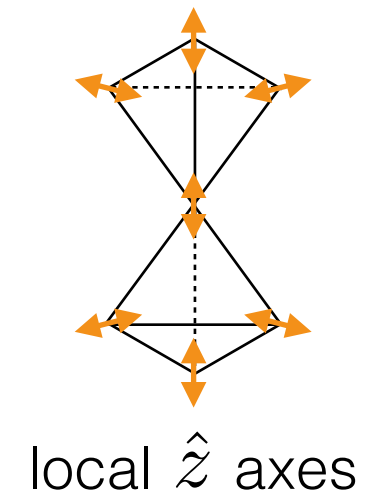
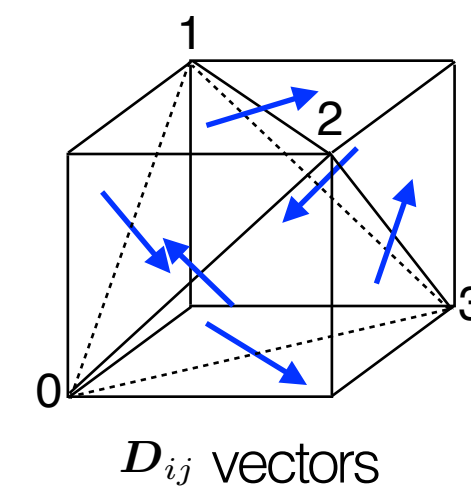
$$H = \sum_{\langle ij \rangle} [JS_i \cdot S_j + D_{ij} \cdot (S_i \times S_j)] + \sum_i D_z (S_i \cdot \hat{z}_i)^2$$

Heisenberg **Dzyaloshinskii-Moriya** **single ion anisotropy**
($J > 0$)

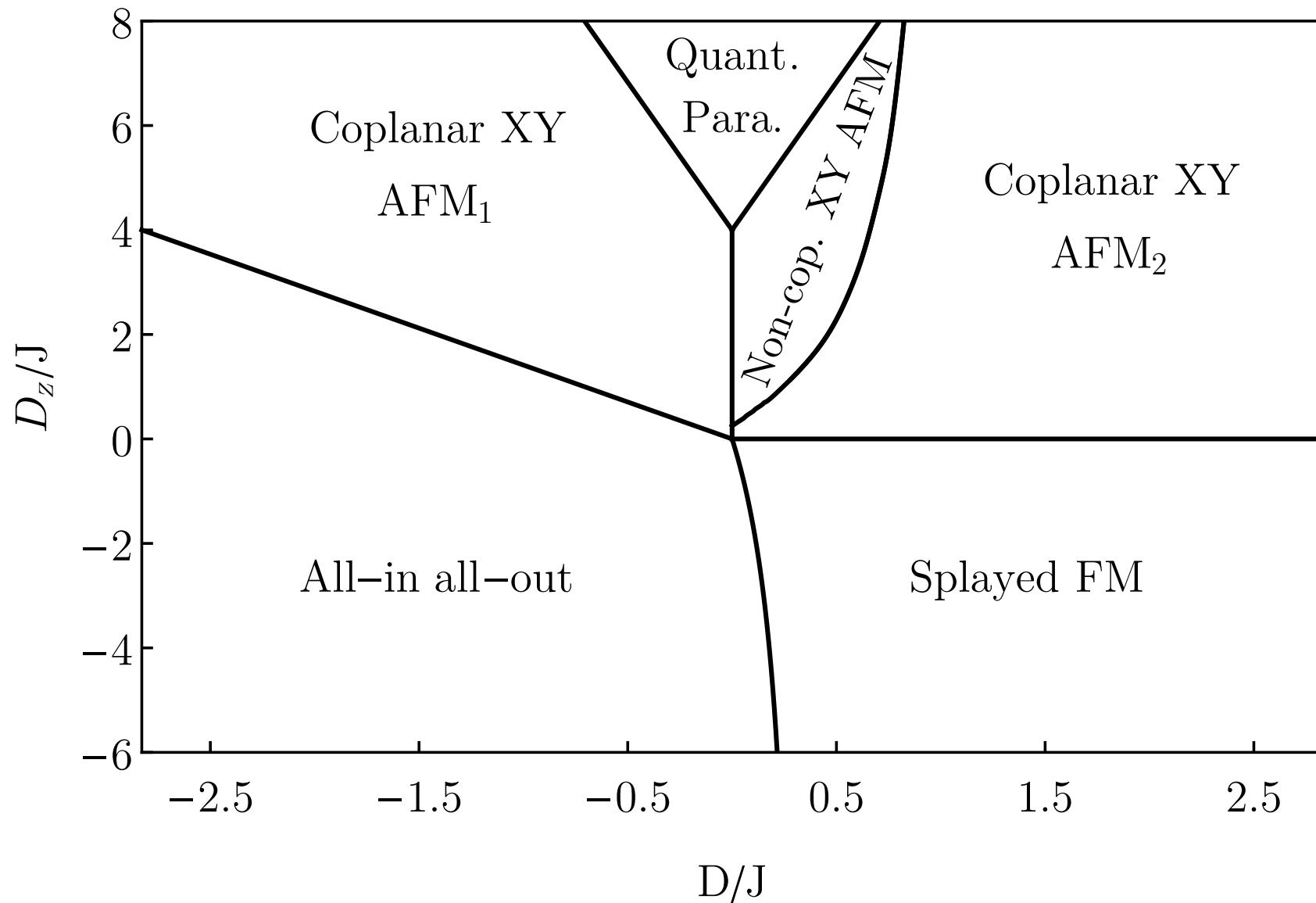
$$|D_{ij}|/J \sim \mathcal{O}(\lambda/\Delta)$$

$$|D_z|/\Delta \sim \mathcal{O}(\lambda^2/\Delta^2)$$

λ : SOC Δ : CEF splitting

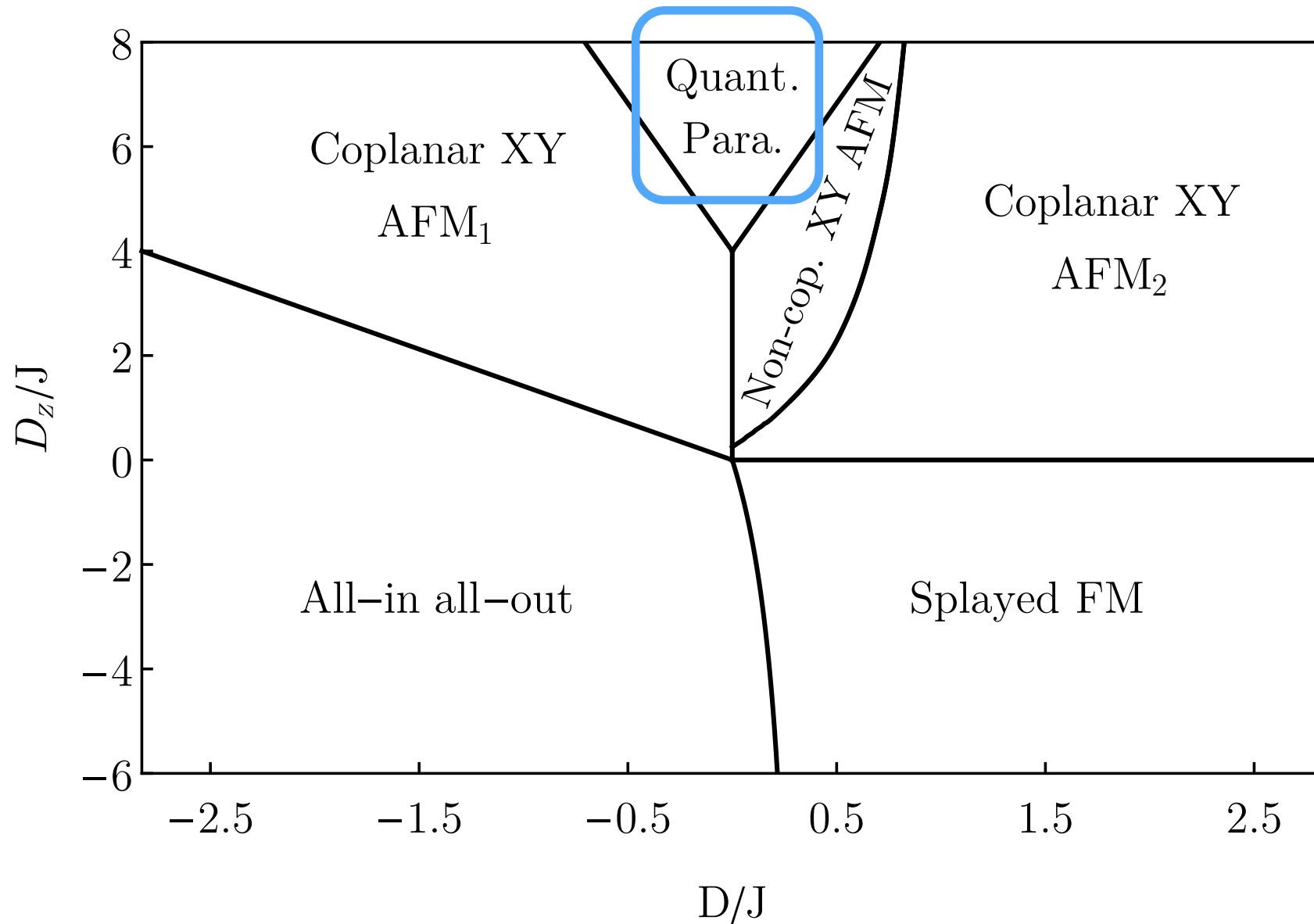


Phase diagram (overview)



Quant. Para. = quantum paramagnetic phase
Others are magnetic ordered phases

Quantum paramagnetic phase



Quant. Para. = quantum paramagnetic phase
Others are magnetic ordered phases

Quantum paramagnetic phase

$D_z \rightarrow +\infty$ (easy plane limit): $|\Psi\rangle = \prod_i |S_i^z \equiv \mathbf{S}_i \cdot \hat{\mathbf{z}}_i = 0\rangle$

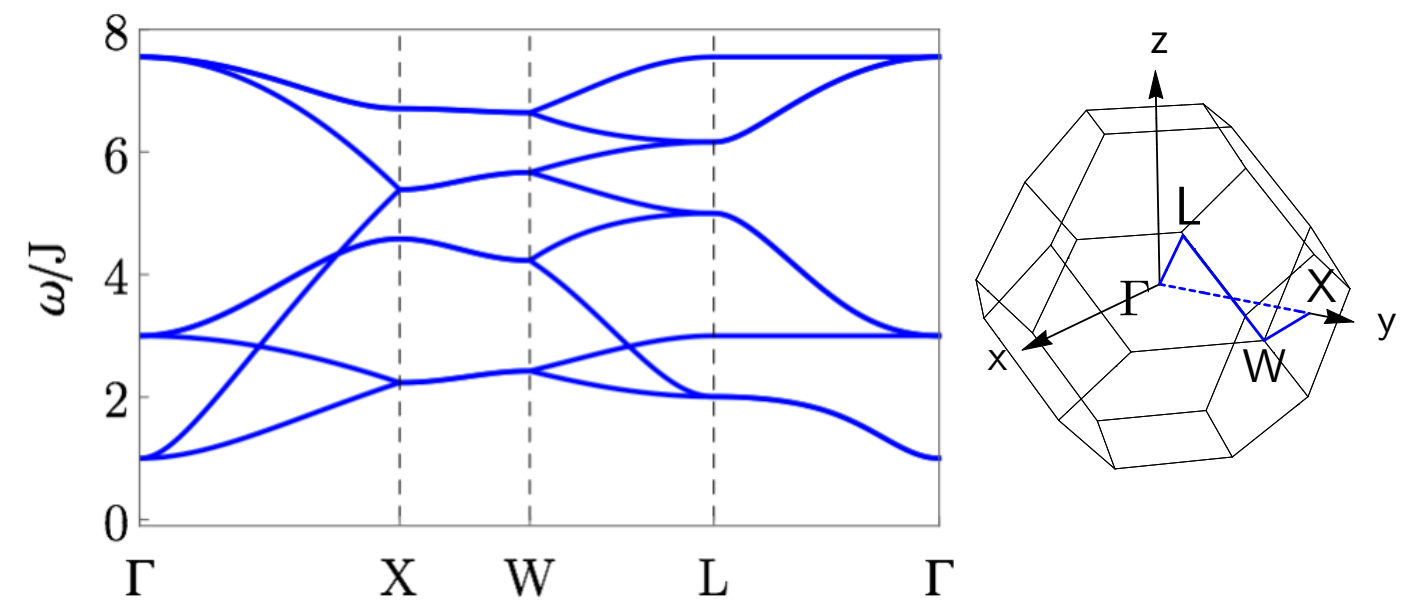
Flavor wave theory

start from the ground state in easy plane limit, one can introduce two flavors of bosons to represent the spin Hamiltonian

$$a_{1(i)}^\dagger |S_i^z = 0\rangle = |S_i^z = 1\rangle$$

$$a_{\bar{1}}^\dagger |S_i^z = 0\rangle = |S_i^z = -1\rangle$$

$$H_{\text{fw}} = \sum_{\mathbf{k}} \Psi_{\mathbf{k}}^\dagger M(\mathbf{k}) \Psi_{\mathbf{k}}$$



flavor wave excitations

8 branches = 4 sublattices x 2 flavors

Quantum paramagnetic phase

$D_z \rightarrow +\infty$ (easy plane limit): $|\Psi\rangle = \prod_i |S_i^z \equiv \mathbf{S}_i \cdot \hat{\mathbf{z}}_i = 0\rangle$

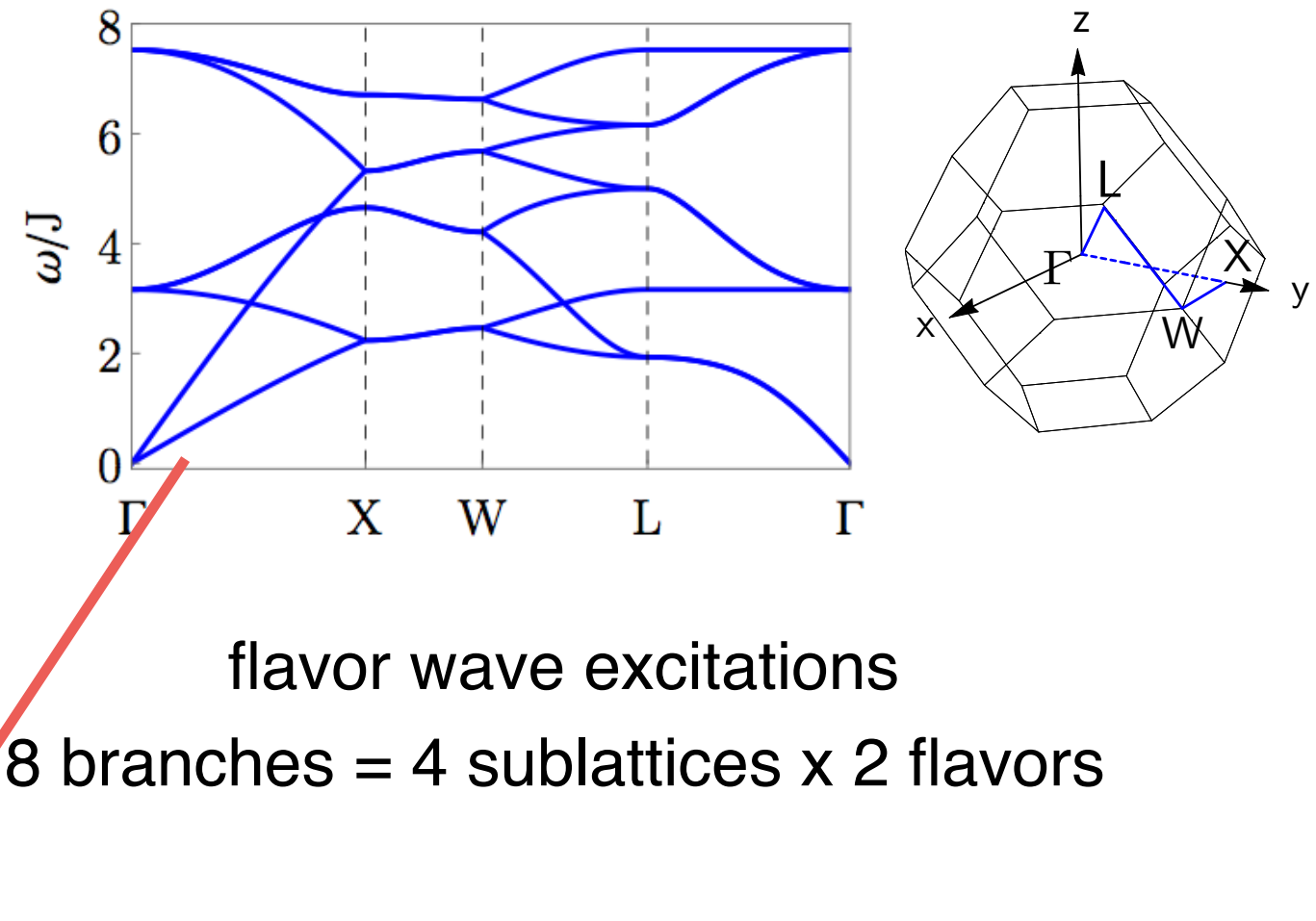
Flavor wave theory

start from the ground state in easy plane limit,
one can introduce two flavors of bosons to
represent the spin Hamiltonian

$$a_{1(i)}^\dagger |S_i^z = 0\rangle = |S_i^z = 1\rangle$$

$$a_1^\dagger |S_i^z = 0\rangle = |S_i^z = -1\rangle$$

$$H_{\text{fw}} = \sum_{\mathbf{k}} \Psi_{\mathbf{k}}^\dagger M(\mathbf{k}) \Psi_{\mathbf{k}}$$

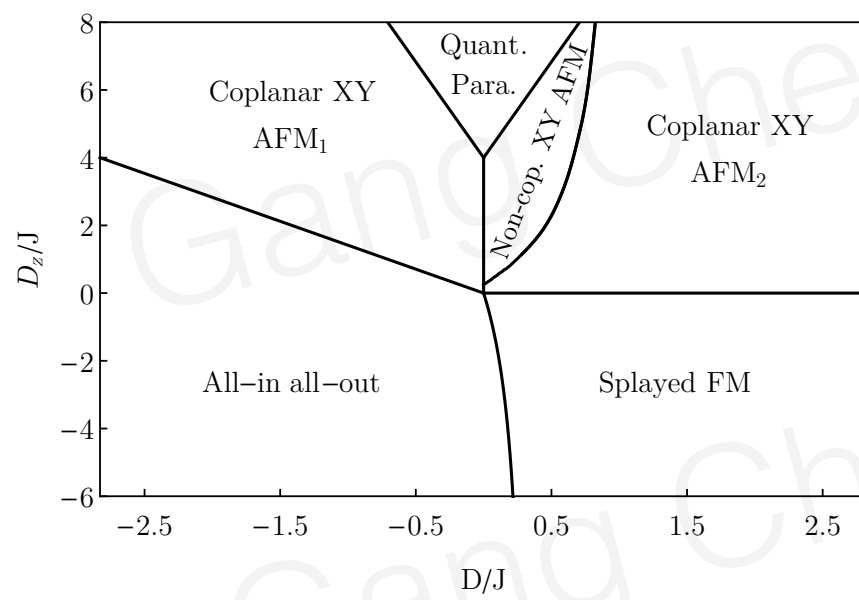


instability of the quantum paramagnet \Rightarrow magnetic order

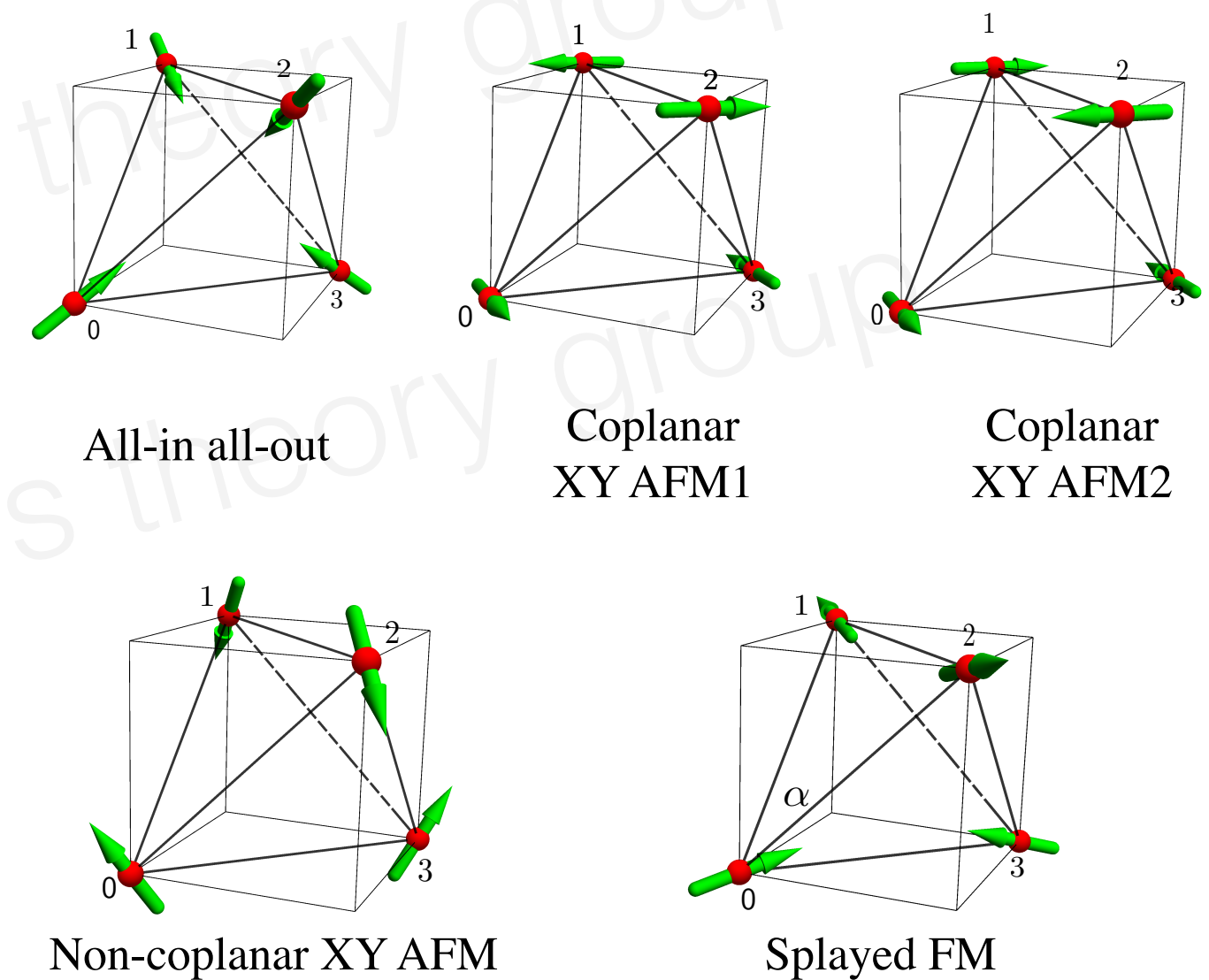
Competing magnetic orders

Mean-field theory

$$\langle H \rangle = \sum_{\langle ij \rangle} J \mathbf{m}_i \cdot \mathbf{m}_j + \mathbf{D}_{ij} \cdot (\mathbf{m}_i \times \mathbf{m}_j) + \sum_i D_z (\mathbf{m}_i \cdot \hat{z}_i)^2$$



All ordered states have $\mathbf{Q}=0$



Magnetic ordered phases

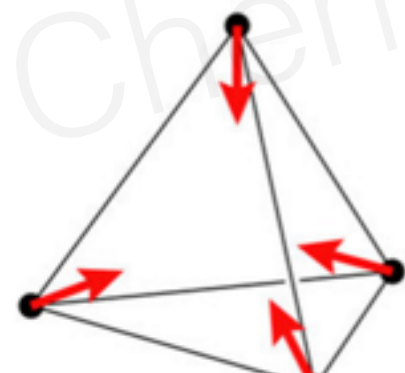
The ordered phases can be understood from degeneracy lifting:

J term requires $\sum_{i \in I_{u/d}} \mathbf{S}_i = 0$ in one tetrahedron (huge degeneracy)



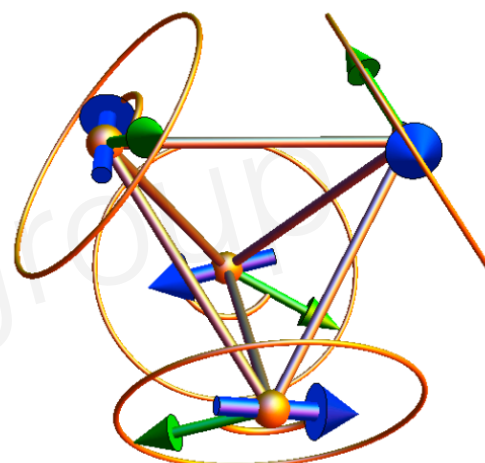
$$-|D| \sum_i (\mathbf{S}_i \cdot \hat{z}_i)^2$$

“Z-type” order:
local Z axis
all-in all-out
two-in two-out



$$|D| \sum_i (\mathbf{S}_i \cdot \hat{z}_i)^2$$

“XY-type” order:
local XY plane

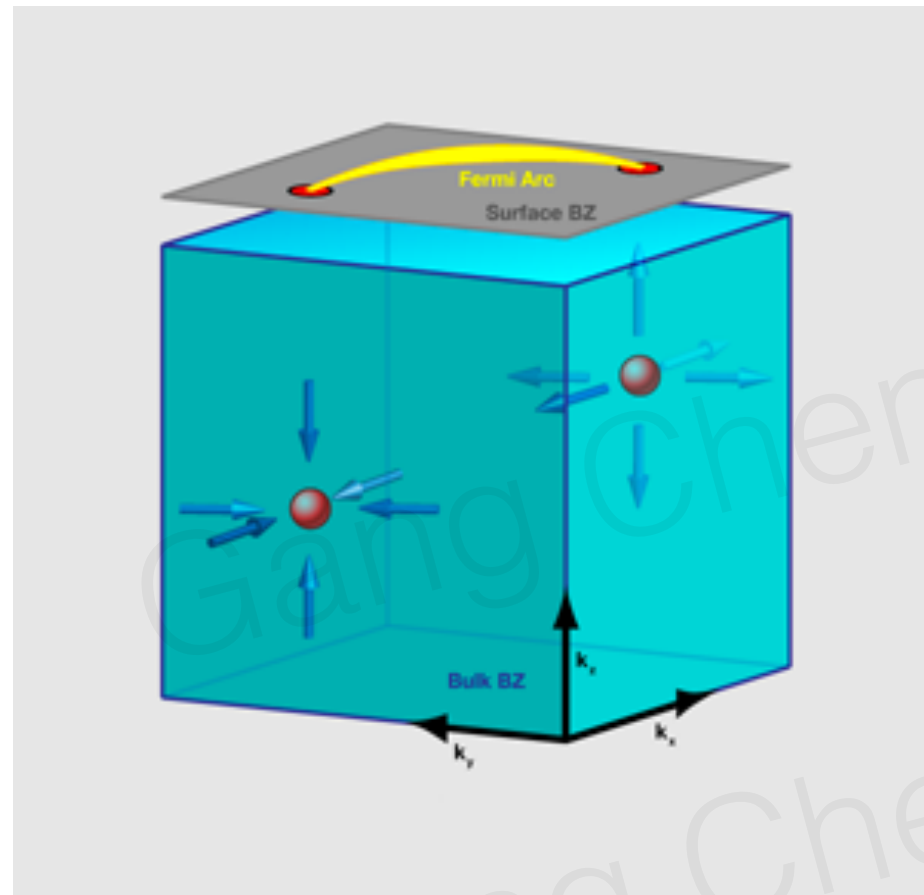


Further selected by the sign of DM interaction
or
Quantum order by disorder

C. L. Henley **J. Appl. Phys.** 1987

L. Savary, K. A. Ross, B. D. Gaulin, J. P. C. Ruff and L. Balents **PRL** 2012

Weyl semimetal and extension

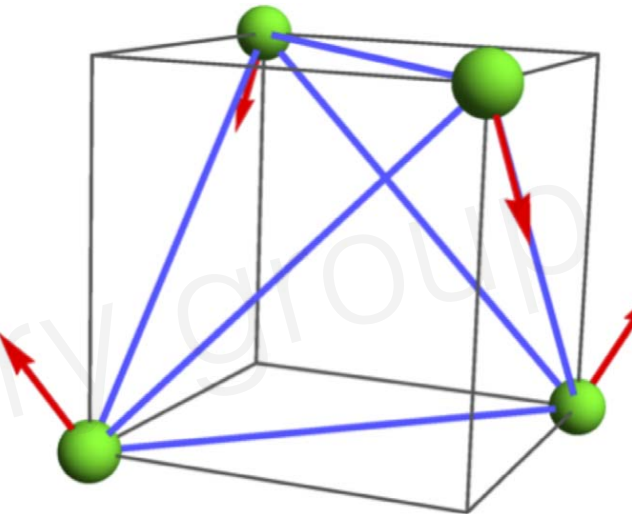
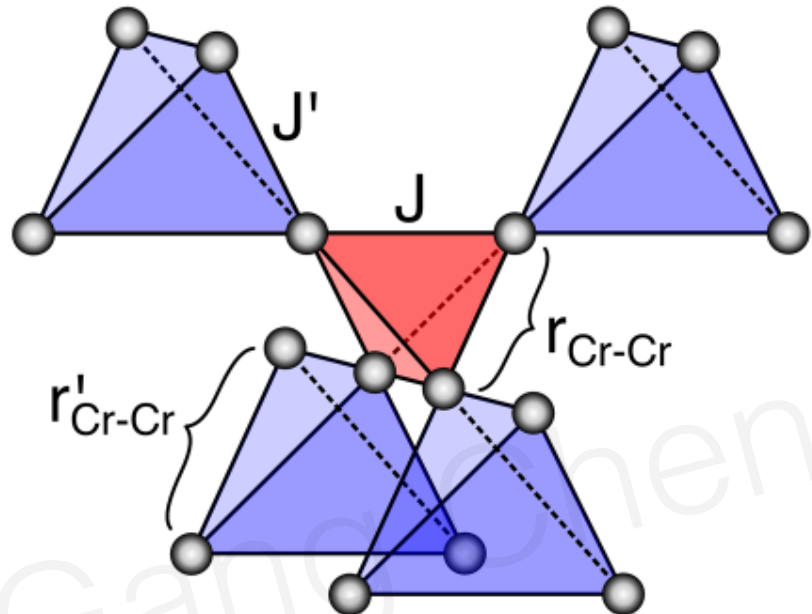


$$H_D = E_0 \mathbb{1} + \mathbf{v}_0 \cdot \mathbf{q} \mathbb{1} + \sum_{i=1}^3 \mathbf{v}_i \cdot \mathbf{q} \sigma_i. \quad (1)$$

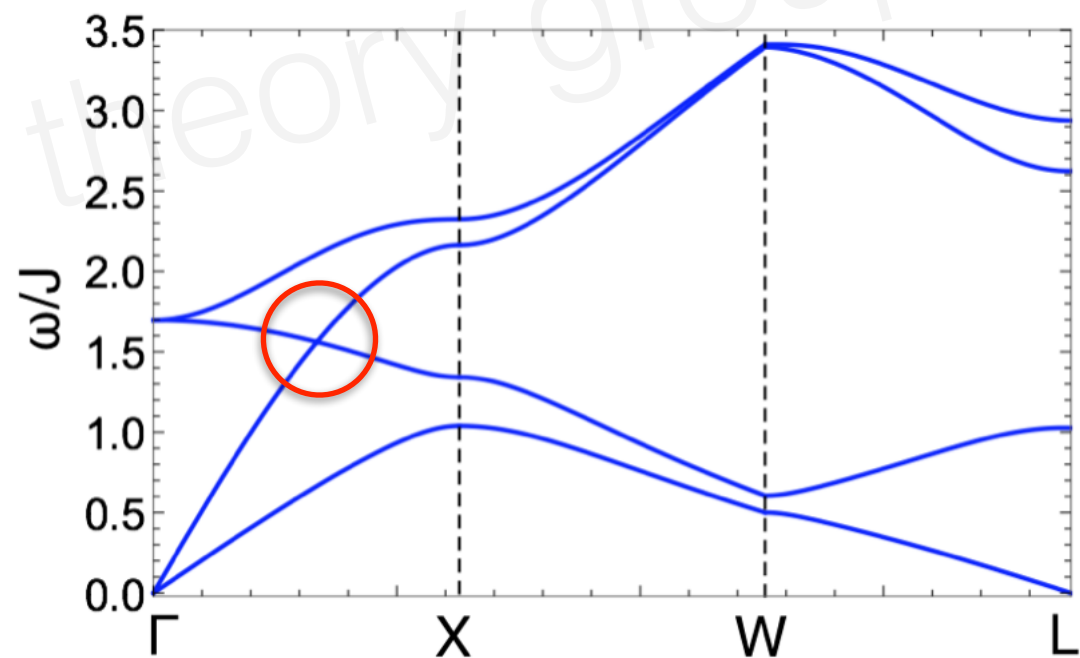
Energy is measured from the chemical potential, $\mathbf{q} = \mathbf{k} - \mathbf{k}_0$

Extension: Type-II Weyl semimetal, Dirac semimetal, nodal line semimetal, hourglass fermion, new fermions

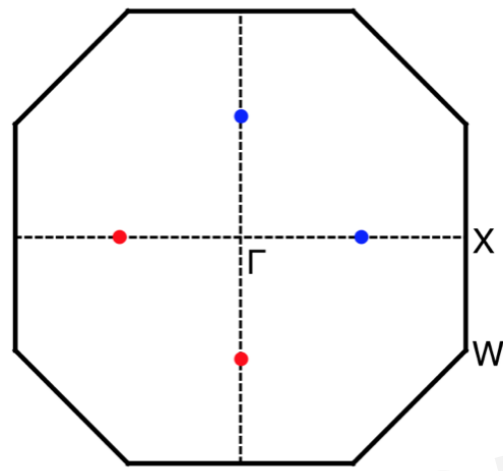
Topological magnons: Weyl magnon



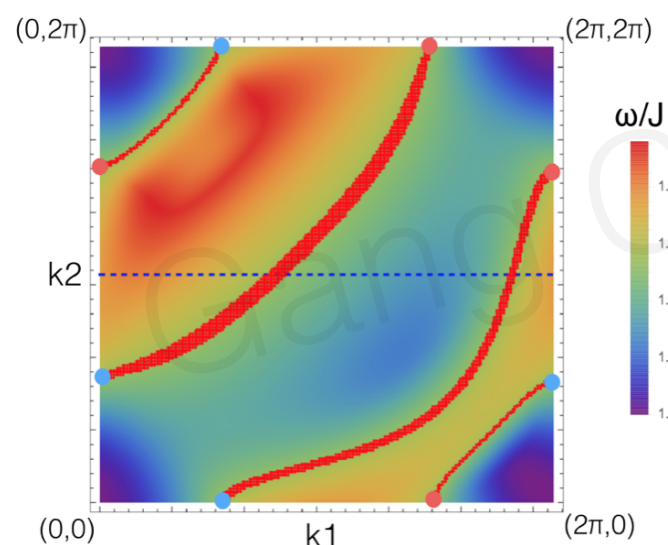
F-Y Li, YD Li, Kim, Balents, Yu, **GC**,
Nature communications 2016



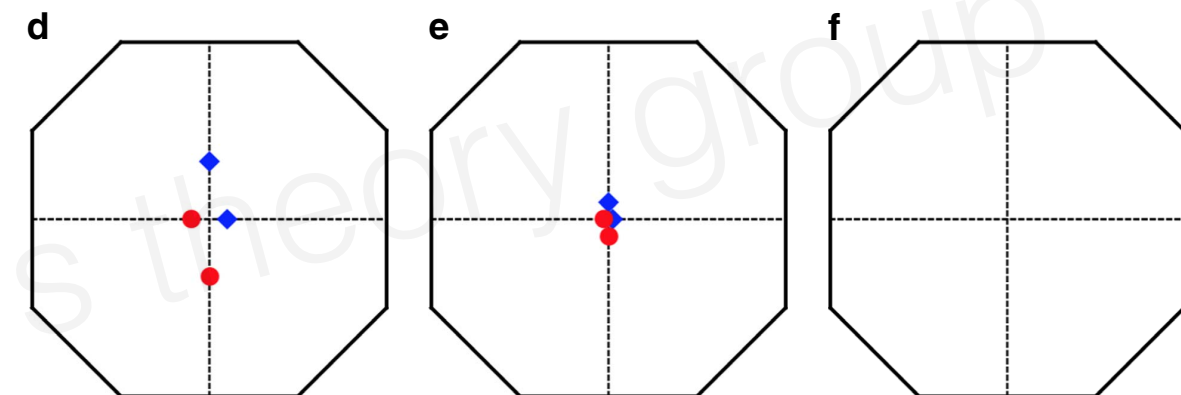
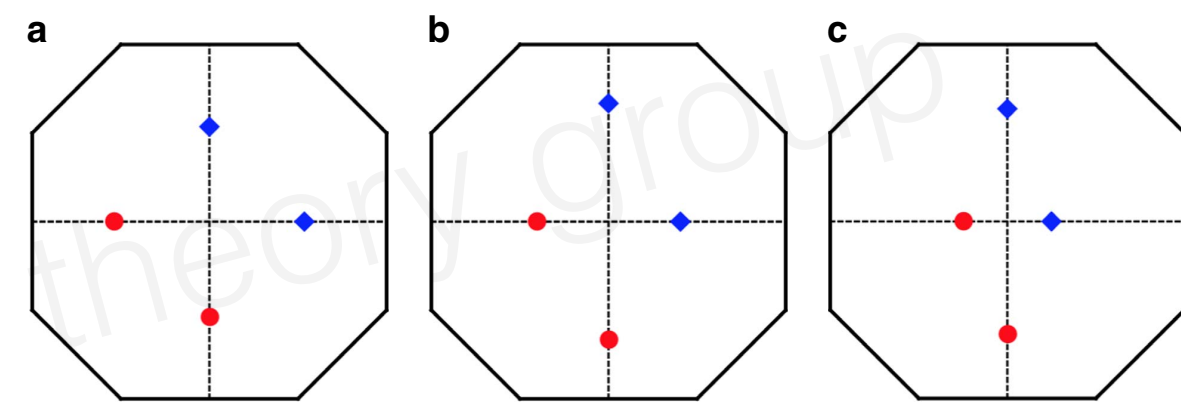
Unique properties of topological Weyl magnon



Magnon Weyl nodes



Magnon surface arcs



tune Weyl nodes with fields

B

Focus session: topological magnons

Monday–Friday, March 4–8, 2019; Boston, Massachusetts

Session Index

Session V44: Topological Magnons

[Show Abstracts](#)

Invited

Room: BCEC 210C

Thursday, March 7, 2019
2:30PM - 3:06PM

[V44.00001: Topological magnon bands in ultra-thin film pyrochlore iridates and iron jarosites](#)
Invited Speaker: Gregory Fiete

Thursday, March 7, 2019
3:06PM - 3:42PM

[V44.00002: Topological spin excitations in a three-dimensional antiferromagnet](#)
Invited Speaker: Yuan Li

Thursday, March 7, 2019
3:42PM - 4:18PM

[V44.00003: Topology of magnons: classification and application to honeycomb Kitaev magnets](#)
Invited Speaker: Yuan-Ming Lu

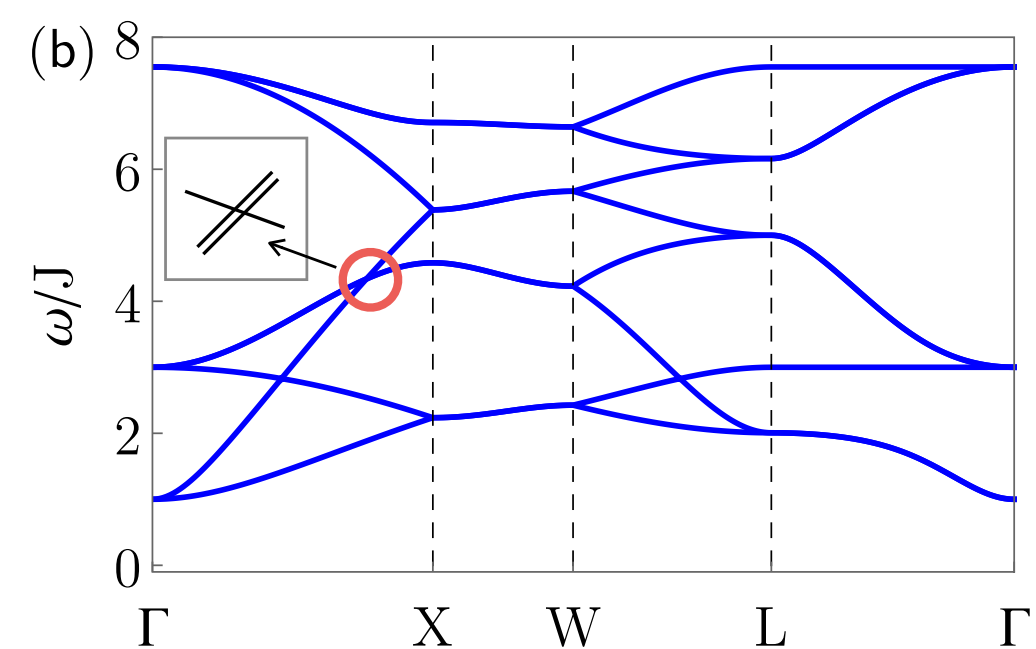
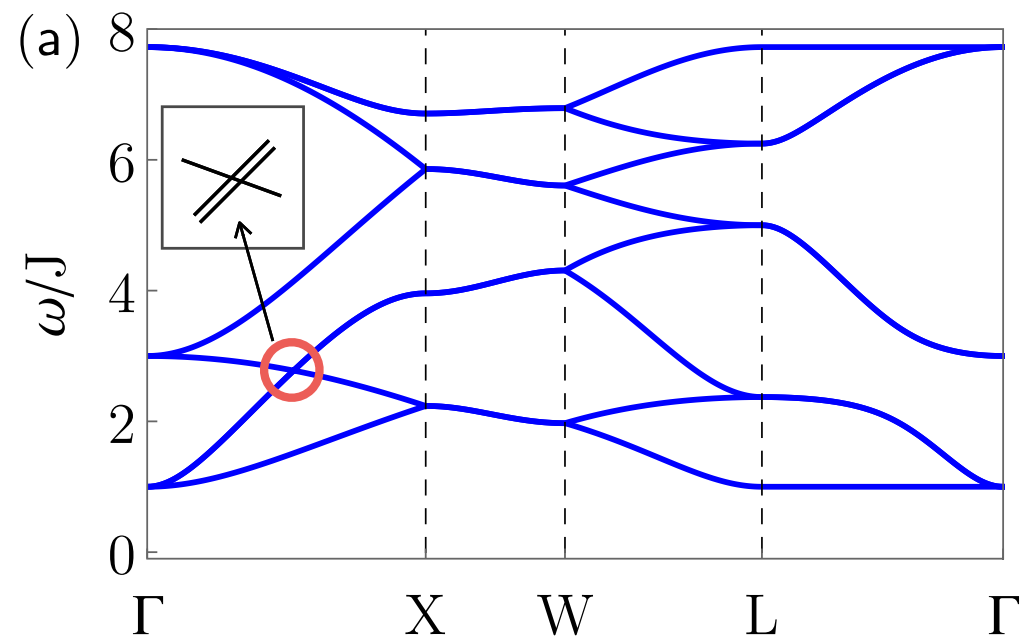
Thursday, March 7, 2019
4:18PM - 4:54PM

[V44.00004: Discovery of coexisting Dirac and triply degenerate magnons in a three-dimensional antiferromagnet](#)
Invited Speaker: Jinsheng Wen

Thursday, March 7, 2019
4:54PM - 5:30PM

[V44.00005: The surprising usefulness of magnons at intermediate and high energies: from frustration to topology](#)
Invited Speaker: Roderich Moessner

Topological magnons for spin-1 pyrochlores



Triple degeneracy

Topological magnons for spin-1 pyrochlores

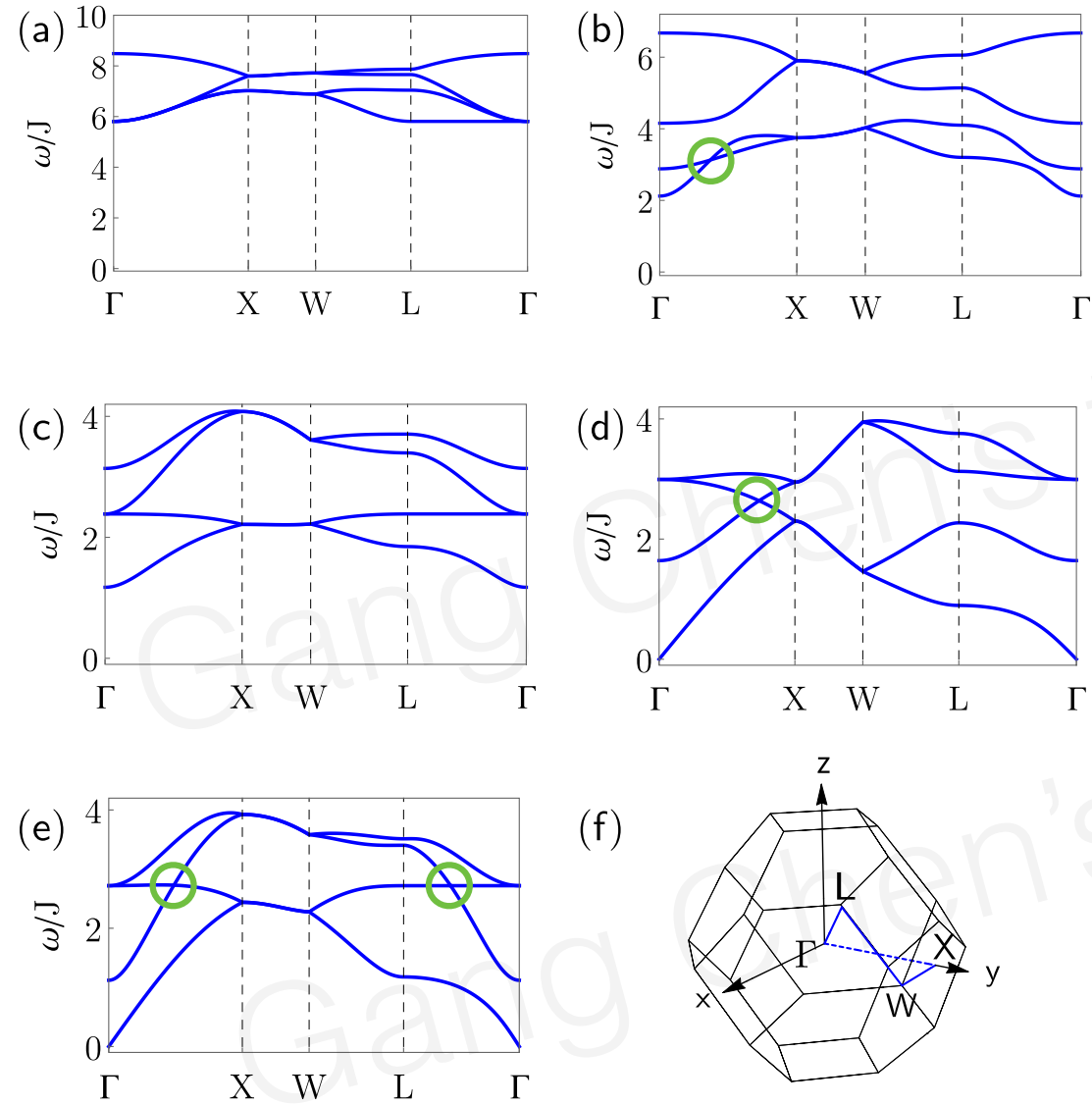


FIG. 7. Spin wave excitations of the ordered phases. The pa-

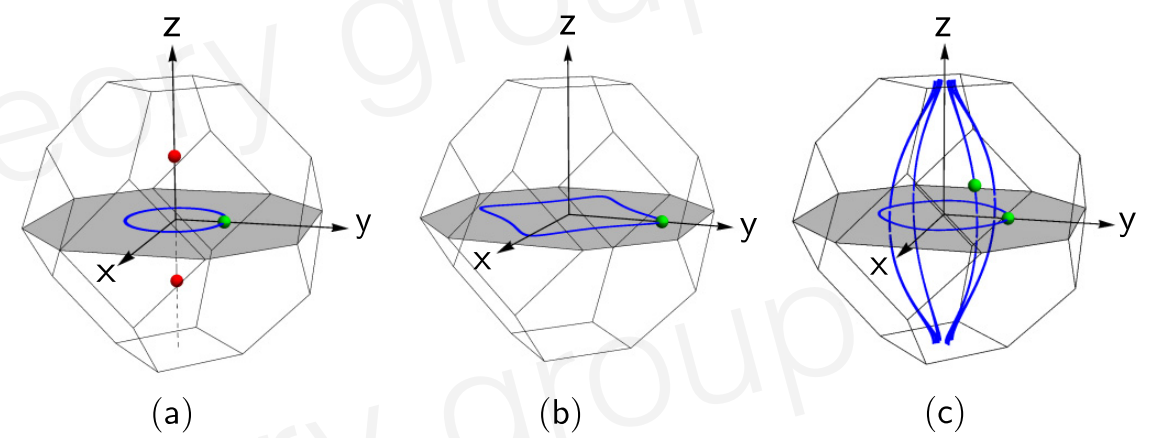
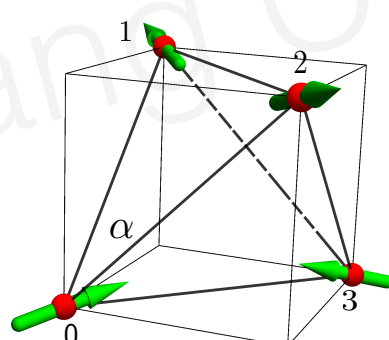


FIG. 8. The nodal lines and Weyl nodes of the spin wave excitation. (a) For the same parameters as in Fig. 7(b), there is a nodal

Materials' relevance

materials	magnetic ions	Θ_{CW}	magnetic transitions	magnetic structure
NaCaNi ₂ F ₇	Ni ²⁺ (3d ⁸)	-129K	glassy transition at 3.6K	spin glass
Y ₂ Ru ₂ O ₇	Ru ⁴⁺ (4d ⁴)	-1250K	AFM transition at 76K	canted AFM $\mathbf{Q} = \mathbf{0}$
Tl ₂ Ru ₂ O ₇	Ru ⁴⁺ (4d ⁴)	-956K	structure transition at 120K	gapped paramagnet
Eu ₂ Ru ₂ O ₇	Ru ⁴⁺ (4d ⁴)	-	Ru order at 118K	Ru order
Pr ₂ Ru ₂ O ₇	Ru ⁴⁺ (4d ⁴), Pr ³⁺ (4f ²)	-224K	Ru AFM order at 162K	Ru AFM order
Nd ₂ Ru ₂ O ₇	Ru ⁴⁺ (4d ⁴), Nd ³⁺ (4f ³)	-168K	Ru AFM order at 143K	Ru AFM order
Gd ₂ Ru ₂ O ₇	Ru ⁴⁺ (4d ⁴), Gd ³⁺ (4f ⁷)	-10K	Ru AFM order at 114K	Ru AFM order $\mathbf{Q} = \mathbf{0}$
Tb ₂ Ru ₂ O ₇	Ru ⁴⁺ (4d ⁴), Tb ³⁺ (4f ⁸)	-16K	Ru AFM order at 110K	Ru AFM order $\mathbf{Q} = \mathbf{0}$
Dy ₂ Ru ₂ O ₇	Ru ⁴⁺ (4d ⁴), Dy ³⁺ (4f ⁹)	-10K	Ru AFM order at 100K	Ru AFM order
Ho ₂ Ru ₂ O ₇	Ru ⁴⁺ (4d ⁴), Ho ³⁺ (4f ¹⁰)	-4K	Ru AFM order at 95K	Ru FM order $\mathbf{Q} = \mathbf{0}$
Er ₂ Ru ₂ O ₇	Ru ⁴⁺ (4d ⁴), Er ³⁺ (4f ¹¹)	-16K	Ru AFM order at 92K	Ru AFM order $\mathbf{Q} = \mathbf{0}$
Yb ₂ Ru ₂ O ₇	Ru ⁴⁺ (4d ⁴), Yb ³⁺ (4f ¹³)	-	Ru AFM order at 83K	Ru AFM order
Y ₂ Mo ₂ O ₇	Mo ⁴⁺ (4d ²)	-200K	Mo spin glass at 22K	Mo spin glass
Lu ₂ Mo ₂ O ₇	Mo ⁴⁺ (4d ²)	-160K	Mo spin glass at 16K	Mo spin glass
Tb ₂ Mo ₂ O ₇	Mo ⁴⁺ (4d ²), Tb ³⁺ (4f ⁸)	20K	spin glass at 25K	spin glass



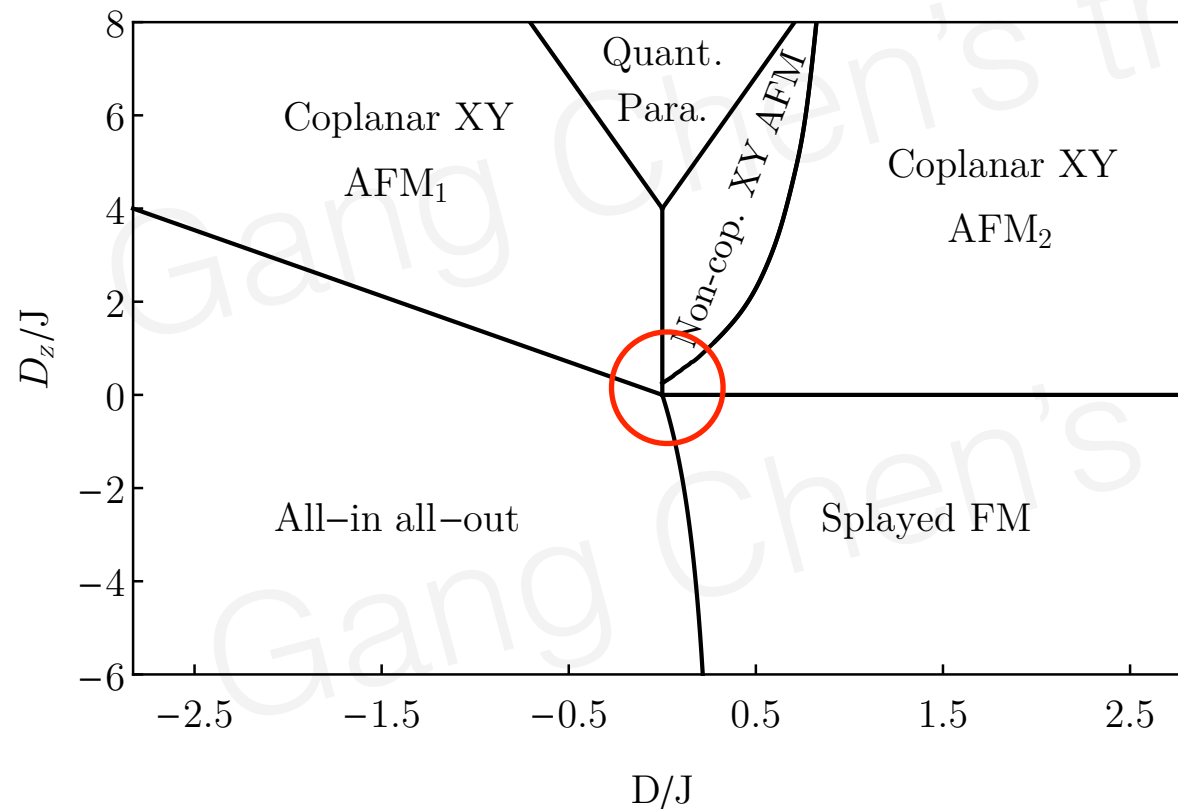
Splayed FM

on the systems with more known results. Ho₂Ru₂O₇ was studied using neutron scattering measurements in a nice paper [109] by C.R. Wiebe *et al.* The authors revealed the Ru moment order at ~ 95 K and the Ho moment order at ~ 1.4 K. The high temperature Ru magnetic order is consistent with the splayed FM with a splayed angle $\alpha \approx 41^\circ$. Under the internal exchange

C. R. Wiebe, J. S. Gardner, S.-J. Kim, G. M. Luke, A. S. Wills, B. D. Gaulin, J. E. Greidan, I. Swainson, Y. Qiu, and C. Y. Jones, *Phys. Rev. Lett.* **93**, 076403 (2004).

Discussion I

The Heisenberg point requires more “quantum” treatment



Heisenberg point $D = 0, D_z = 0$

classical ground states are
extensively degenerate

strong quantum fluctuations
and
fundamental distinctions
between spin-1/2 and spin-1

Discussion II

Relation to spin-3/2 pyrochlores:

- The same model actually applies to the spin-3/2 pyrochlore materials (e.g. [Mn-based pyrochlores](#))
- Local spin anisotropy acts on it quite differently, $D_z(S_i \cdot \hat{z}_i)^2$
The quantum paramagnetic phase is absent since no Sz=0 state.
- The magnetic orders, if they occur, would be similar to the spin-1 pyrochlore system. The magnetic excitations would have similar properties, too.



Fei-Ye Li
Fudan

Summary

1. We propose a minimal spin model for spin-1 pyrochlores
2. The competing phases and topological excitations are discussed.
3. Various materials' realization and relevance are clarified.

Fei-Ye Li, GC, PRB 98, 045109 (2018)